Formation of Ordered Nanostructures in Epoxy Thermosets: A Mechanism of Reaction-Induced Microphase Separation

Fanliang Meng,[†] Sixun Zheng,*[,†] Huiqin Li, Qi Liang,*[,‡] and Tianxi Liu[§]

Department of Polymer Science and Engineering, Shanghai Jiao Tong University, Shanghai 200240, China, Instrumental Analysis Center, Shanghai Jiao Tong University, Shanghai 200240, China, and Laboratory of Advanced Materials, Fudan University, Shanghai 200433, China

Received January 2, 2006; Revised Manuscript Received May 23, 2006

ABSTRACT: A polystyrene-*b*-poly(ethylene oxide) (PS-*b*-PEO) diblock copolymer was synthesized via the atom transfer radical polymerization (ATRP) of styrene with mono-2-bromoisobutyryl-terminated PEO [PEO−$OOCCBr(CH_3)_2$] as a macroinitiator, and the polymerization was mediated by copper(I) bromide (CuBr) and 2,2′-bipyridine (BPY). The PS-*b*-PEO diblock copolymer was used to incorporate into epoxy resin to afford the nanostructured epoxy thermosets. Both atomic force microscopy (AFM) and small-angle X-ray scattering (SAXS) showed that the long-range ordered nanostructures were obtained via the approach of in situ polymerization in the presence of the diblock copolymer. It was found that the nanophases of PS were arranged into a simple cubic symmetry lattice while the content of diblock copolymer was 40 wt %. In view of the difference in miscibility and phase behavior for the blends of the subchains (i.e., PS and PEO) of the diblock copolymer with epoxy after and before curing, the formation of the ordered nanostructures was judged to be via the mechanism of reaction-induced microphase separation, which is in marked contrast to the mechanism of self-organization of block copolymers together with the subsequent fixation of the self-organized structures.

Introduction

The morphological control of thermosets at the nanometer level is long a pursuit in the studies of polymer materials;[1,2] the formation of nanostructures in thermosets can further optimize the properties of materials. It is crucial to understand the formation mechanisms of nanostructures in thermosets for controlling the morphology to obtain the improved properties of the materials. de Gennes[3,4] proposed that ordered nanostructures of thermosets can be formed via locking in preformed ordered mesoscopic structures of thermosets precursors via polymerization (i.e., cross-linking). As one of the successful applications, liquid-crystalline epoxy resins have been developed to obtain the materials with ordered mesomorphic structures, which thus endow the materials with improved properties.[5−11] More recently, Bates et al.[12,13] proposed a novel strategy of creating the nanostructures in thermosets using amphiphilic block copolymers. In the protocol, precursors of thermosets act as selective solvents of block copolymers and some self-assembly morphology, such as lamellar, bicontinuous, cylindrical, and spherical structures, are formed in the mixtures depending on blend composition before curing reaction. The micelle structures can be fixed with adding hardeners and subsequent curing. During the past years, a variety of block copolymer architectures have been used to obtain some equilibrium ordered (or disordered) nanostructures thermosets based on this strategy.[14−28] In this method, the role of curing reaction is to lock in the morphology that is already present, although it was identified that there were some small changes in the nanostructures after and before the curing reaction.[12,13]

The prerequisite for the self-assembly approach is that block copolymers are self-organized into micelle structures in their mixtures with precursors of thermosets prior to curing. Nonetheless, this case does not always occur because, in many circumstances, all the subchains of block copolymers are miscible with the precursors of thermosets. The miscibility (or solubility) is ascribed to the negligible entropic contribution (ΔS_m) to free energy of mixing (ΔG_m) in the mixtures of block copolymers and the low molecular compounds (viz., precursor of thermosets).[1,29] In addition, the presence of the self-organized microphases formed at lower temperatures does not purport the survival of the structures at elevated temperatures that are required for the curing of some high-performance thermosets. It has been known that the mixtures of polymers with precursors of thermosets generally displayed upper critical solution temperature (UCST) behaviors.[1,29] Under this circumstance, it is proposed that the nanostructured thermosets can alternatively be able to prepare via the approach of reaction-induced microphase separation, i.e., the nanostructures can be accessed by controlling the microphase separation of a part of subchains of block copolymers induced by polymerization, whereas the other subchains remain miscible with the cross-linked thermosets. In the previous work, we have shown that the nanostructured thermosets can successfully be prepared via the reaction-induced microphase separation mechanism.[30] Nonetheless, the question has not been well answered whether some long-range ordered nanostructures could be obtained via the reaction-induced microphase separation mechanism or not. It is proposed that the formation of nanostructures in the reaction-induced microphase separation system could be governed by the following two aspects of factors: (i) the competitive kinetics (or dynamics) between phase separation and polymerization, and (ii) the confinement of the miscible subchains on microphase-separated subchains of block copolymers. It has been known that, in the thermosetting blends containing homopolymers (and/or random copolymers), fine morphological structures can be formed via spinodal decomposition (SD) (and/or nucleation and growth, NG) mechanism.[1] In the case of the thermosets containing block copolymers, the surface tension (or

* To whom correspondence should be addressed. E-mail: szheng@sjtu.edu.cn (S.Z.); qiliang@sjtu.edu.cn (Q.L.). Telephone: 86-21-54743278. Fax: 86-21-54741297.

[†] Department of Polymer Science and Engineering, Shanghai Jiao Tong University.

[‡] Instrumental Analysis Center, Shanghai Jiao Tong University.

[§] Laboratory of Advanced Materials, Fudan University.

10.1021/ma060004+ CCC: $33.50
Published on Web 06/28/2006

free energy) of domains of separated subchains will be reduced due to the presence of miscible subchains of the block copolymer. It is expected that ordered nanostructures should be able to be obtained if the separated nanophases are densely packed in the systems, which can readily be detected by means of microscopy (e.g., TEM, AFM) and small-angle X-ray scattering (SAXS). To the best of our knowledge, however, the study remains largely unexplored.

The purpose of this work is to demonstrate that long-range ordered nanostructures can be accessed via the reaction-induced microphase separation approach. To this end, an amphiphilic diblock copolymer, polystyrene-*block*-poly(ethylene oxide) (PS-*b*-PEO) was synthesized to incorporate into epoxy resin by knowing that: (i) PEO subchain is miscible with epoxy after and before the curing reaction, (ii) the blends of PS block with epoxy precursor exhibited an upper critical solution temperature (UCST) behavior and the reaction-induced phase separation occurs when the blends are cured above the UCST. Atomic force microscopy (AFM) and small-angle X-ray scattering (SAXS) were used to examine the ordered nanostructures formed via the reaction-induced microphase separation, and the formation of nanostructures in the thermosets is addressed based on the reaction-induced microphase separation mechanism.

Experimental Section

Materials. The epoxy monomer used in this work is diglycidyl ether of bisphenol A (DGEBA) with an epoxide equivalent weight of 185−210, supplied by Shanghai Resin Co., China. 4,4′-Methylenebis(2-chloroaniline) (MOCA) is of chemically pure grade and was used as the curing agent, purchased from Shanghai Reagent Co., Shanghai, China. Styrene (St) is of analytically pure grade and was purchased from Shanghai Reagent Co., China. Prior to use, the inhibitor was removed by washing with aqueous sodium hydroxide (5 wt %) and deionized water for at least three times and dried by anhydrous Na_2SO_4; the monomer was further distilled at reduced pressure. 2-Bromoisobutyryl bromide was purchased from Aldrich Co. USA and used as received. Copper(I) bromide (CuBr) was purchased from Shanghai Reagent Co., China, and it was purified according to the reported procedure.[31] *S*-benzyl dithiobenzoate (BDB) was prepared by following the litureature method,[32] which was used as a chain transfer agent for the reversible addition−fragmentation transfer (RAFT) polymerization of sytrene. Poly(ethylene oxide) monomethyl ether (MPEO5000) with a quoted molecular weight of $M_n = 5000$ was purchased from Fluka Co., Gernany, and it was dried by azeotropic distillation with toluene prior to use. 2,2′-Bipyridine (BPY) was supplied by Shanghai Reagent Co., China, and used as received. The solvents such as tetrahydrofuran (THF), dichloromethane, petroleum ether (distillation range: 60−90 °C), and triethylamine (TEA) were of analytically pure grade, obtained from commercial resources. Prior to use, triethylamine (TEA) was dried over CaH_2 and then was refluxed with *p*-toluenesulfonyl chloride, followed by distillatuion. Dichloromethane (CH_2Cl_2) was purified with concentrated H_2SO_4 until the acid layer became colorless and then was washed with aqueous $NaHCO_3$ (5 wt %) and deionized water. Finally, it was distilled over CaH_2. All other solvents were used as received unless specified.

Synthesis of Polystyrene. Polystyrene with the same molecular weight as the PS subchain in the diblock copolymer was synthesized by means of RAFT polymerization of sytrene in the presence of azobis(isobutyronitrile) (AIBN) with *S*-benzyl dithiobenzoate (BDB)[32] as the chain transfer agent (CTA). The bulk polymerization of styrene was carried out in an ampule. Typically, styrene (10.2 g, 0.08 mol), BDB (0.4562 g, 0.0018 mol), and AIBN (0.074 g, 0.0043 mol) were charged to the ampule, and the reactive system was degassed by three freeze−pump−thaw cycles and the polymerization was carried out at 70 °C for 24 h. At the end of the reaction, the system was cooled to room temperature and diluted with tetrahydrofuran (THF). The solution was then droped into an excessive amount of petroleum ether to afford the precipitates. The product was dried in vacuo at room temperature for 24 h. Gel permeation chromatography (GPC, relative polystyrene standard): $M_n = 7500$, $M_w/M_n = 1.06$.

Synthesis of Diblock Copolymer by Atom Transfer Radical Polymerization. To synthesize PS-*b*-PEO diblock copolymer by means of atom transfer radical polymerization (ATRP), poly(ethylene oxide) macroinitiator was first prepared by following the literature method.[33] In this work, the poly(ethylene oxide) monomethyl ether with a quoted molecular weight of $M_n = 5000$ was used to react with 2-bromoisobutyryl bromide in the presence of triethylamine to afford the 2-bromoisobutyryl-ended PEO [PEO−OOCCBr$(CH_3)_2$]. The synthesis of diblock PS-*b*-PEO was carried out by using a standard Schlenk line system. To a flask connected with the Schlenk line PEO-Br macroinitiator ($M_n = 5000$, 5.0 g, 1.0 mmol), CuBr (0.1455 g, 1.0 mmol), BPY (0.47 g, 3.0 mmol), and styrene (10.0 g, 0.0962 mol) were charged. The reactive mixture was degassed via three pump−freeze−thaw cycles and then immersed in a thermostated oil bath at 110 °C. After the polymerization was carried out for 24 h, the system was cooled to room temperature. Dichloromethane was added to dissolve the product. After filtering over a column of neutral alumina to remove the catalyst, the solution was dropped into an excessive amount of petroleum ether to afford the precipitates. The PS-*b*-PEO diblock copolymer was obtained and dried in a vacuum oven at room temperature for 24 h. The polymer (11.034 g) was obtained with a conversion of 60% for styrene monomer. Fourier transform infrared spectroscopy (FTIR) (KBr window): 2928 (C−H, methylene of PEO), 1108 (C−O−C, ether of PEO), 1600, 1580, 1500, and 1450 (C═C of aromatic rings), 2922 (C−H of PS), 3110−3010 (═C−H of aromatic rings). The ^{1}H nuclear magnetic resonance spectroscopy (NMR) ($CDCl_3$, ppm): 6.30−7.32 (protons of aromatic rings, 5**H**); 3.61 (−OC**H**$_2$C**H**$_2$−, 4**H**); 1.29−2.12 (protons of methylene and methane of PS subchain, 3**H**). According to the integration intensity of PEO protons to that of PS, the molecular weight of copolymer was calculated to be $M_n = 12\,600$. The curve of gel permeation chromatography (GPC, relative polystyrene standard) displayed an unimodal peak, and the molecular weight of $M_n = 15\,600$ and $M_w/M_n = 1.03$ was determined relative to polystyrene standard.

Preparation of DGEBA/PS Blends. The blends of DGEBA with the polystyrene with the same molecular weight as the PS subchain in PS-*b*-PEO were prepared by solution casting from tetrahydrofuran (THF) at room temperature. The concentration was controlled within 5% (w/v). To remove the residual solvent, all the blend films were further desiccated in vacuo at 50 °C for 48 h.

Preparation of Nanostructured Epoxy Resin. The diblock copolymer, PS-*b*-PEO was added to DGEBA at ambient temperature with continuous stirring until the diblock copolymer was completely dissolved. Then the curing agent, MOCA, was added to system with vigorously stirring until homogeneous blends were obtained. The ternary mixture was poured into Teflon moulds and cured at 150 °C for 2 h plus 180 °C for 2 h to access a complete curing reaction. The thermosetting blends containing PS-*b*-PEO up to 50 wt % were obtained.

Scheme 1. Synthesis of PS-*b*-PEO Diblock Copolymer

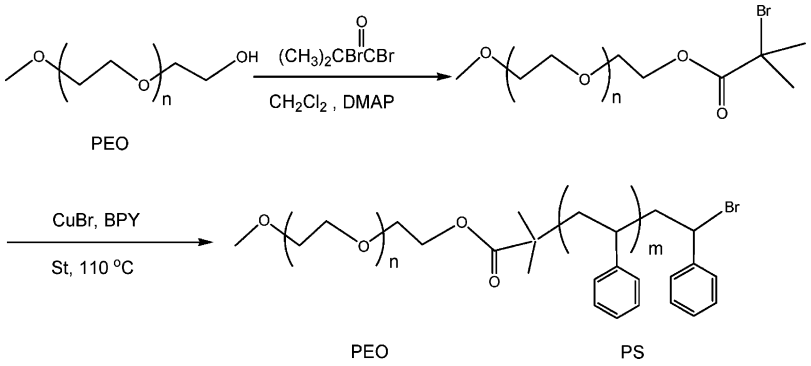

Measurement and Characterization. *Fourier Transform Infrared Spectroscopy (FTIR).* A Perkin-Elmer Paragon 1000 Fourier transform spectrometer was used to measure infrared spectra at room temperature (25 °C). To obtain the FTIR spectrum of PS-*b*-PEO, the diblock copolymer was dissolved with THF and the solution was cast onto a KBr window. The solvent was removed in vacuo at 60 °C for 30 min. The specimens of thermosets were granulated, and the powder was mixed with KBr pellets to press into the small flakes for measurements. All of the specimens were sufficiently thin to be within a range where the Beer−Lambert law is obeyed. In all cases, 64 scans at a resolution of 2 cm^{-1} were used to record the spectra.

Nuclear Magnetic Resonance Spectroscopy (NMR). The ^1H NMR measurements were carried out on a Varian Mercury Plus 400 MHz NMR spectrometer at 25 °C. The samples were dissolved with deuteronated chloroform, and the solutions were measured with tetramethylsilane (TMS) as the internal reference.

Optical Microscopy (OM). A Leica DMLP polarized optical microscope equipped with a hot stage (Linkam TH960, Linkam Scientific Instruments, Ltd., U.K.) with a precision of ±0.1 °C was used for the determination of cloud point temperature (T_{cp}) of the DGEBA/PS mixture. The THF solutions of the mixtures were cast onto cover glasses; the majority of solvent was removed at 50 °C, and the residual solvent was further eliminated in vacuo at 50 °C for 2 h. The films of the blends were sandwiched between two cover glasses. To measure the cloud point curve (CPC), the blend films with various compositions were observed under the polarizing microscope in which the angle between the polarizer and analyzer was 45°.[34] The samples were heated through the cloud points at a rate of 5 °C/min; temperature was increased until a homogeneous solution was obtained. The cloud point was defined as the initial temperature of the turbidity. The cloud points were plotted as a function of blend composition.

Differential Scanning Calorimetry (DSC). Differential scanning calorimetry (DSC) was carried out with a Perkin-Elmer Pyris 1 differential scanning calorimeter in a dry nitrogen atmosphere. An indium standard was used for temperature and enthalpy calibrations, respectively. All of the samples (about 8.0 mg in weight) were first heated to 180 °C and held at this temperature for 3 min to remove the thermal history, followed by quenching to −60 °C. A heating rate of 20 °C/min was used at all cases. Glass transition temperature (T_g) was taken as the midpoint of the heat capacity change. The crystallization temperatures (T_c) and the melting temperatures (T_m) were taken as the temperatures of the minimum and the maximum of both endothermic and exothermic peaks, respectively.

Scanning Electron Microscope (SEM). To observe the phase structure of epoxy blends, the samples were fractured under cryogenic conditions using liquid nitrogen. The fractured surfaces so obtained were immersed in tetrahydrofuran at room temperature for 30 min. The PS phases could be preferentially etched by the solvent, while the epoxy matrix phase remains unaffected. The etched specimens were dried to remove the solvents. The fractured surfaces were coated with thin layers of gold of about 100 Å. All specimens were examined with a Hitachi S210 scanning electron microscope (SEM) at an activation voltage of 15 kV.

Small-Angle X-ray Scattering (SAXS). The SAXS measurements were taken on a Bruker Nanostar system. Two-dimensional diffraction patterns were recorded using an image-intensified CCD detector. The experiments were carried out at room temperature (25 °C) or elevated temperatures using Cu Kα radiation ($\lambda = 1.54$ Å, wavelength) operating at 40 kV, 35 mA. The intensity profiles were output as the plot of scattering intensity (I) versus scattering vector, $q = (4\pi/\lambda)\sin(\theta/2)$ (θ = scattering angle).

Atomic Force Microscopy (AFM). The thermosets samples were trimmed using a microtome machine, and the specimen sections (ca. 70 nm in thickness) were used for AFM observations. The AFM experiments were performed with a Nanoscope IIIa scanning probe microscope (Digital Instruments, Santa Barbara, CA). Tapping mode was employed in air using a tip fabricated from silicon (125 μm in length with ca. 500 kHz resonant frequency). Typical scan speeds during recording were 0.3−1 line × s^{-1} using scan heads with a maximum range of 16 μm × 16 μm.

Results and Discussion

Synthesis of PS-*b*-PEO Diblock Copolymer. The PS-*b*-PEO diblock copolymer was synthesized by ATRP of styrene, which was initiated with 2-bromoisobutyryl-terminated PEO monomethyl ether [MeO−PEO−OOCCBr$(CH_3)_2$]. The synthetic route of the diblock copolymer is shown in Scheme 1. The macroinitiator was prepared via the reaction between poly(ethylene oxide) monomethyl ether [CH_3−(−O−CH_2−CH_2−)$_n$−CH_2−CH_2−OH] and 2-bromoisobutyryl bromide in the presence of triethylamine. The conversion of styrene was controlled within 60% to obtain the copolymer with desired molecular weight. The FTIR results indicate that the as-synthesized polymer combined the structural features of PEO and PS, which was further confirmed by nuclear magnetic resonance spectroscopy (NMR). Figure 1 presents the ^1H NMR spectrum of the diblock copolymer together with the assignment of the spectrum. The ratio of the integration intensity of protons in aromatic rings to protons of the PEO moiety can be employed to estimate the content of PS subchain to be 60%, which is close to the theoretical value of 62% estimated from the conversion of styrene monomer. The GPC trace of the product

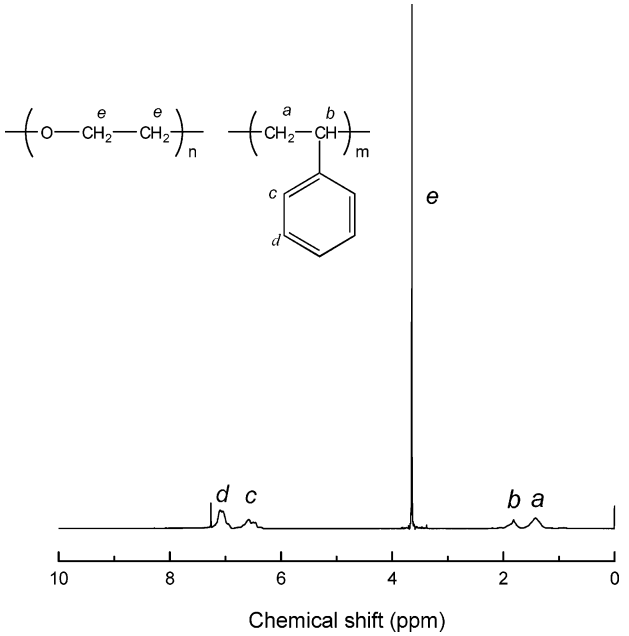

Figure 1. ^{1}H NMR spectrum of PS-*b*-PEO diblock copolymer.

displayed a unimodal peak, indicating that there were no homopolymers in the as-prepared diblock copolymer. From the ratio of the integration intensities of PS to those of PEO protons in the ^{1}H NMR spectrum, the molecular weight of the diblock copolymer was calculated to be $M_n = 12\,600$. Therefore, the lengths of the subchains of the diblock copolymer were $M_n = 5000$ for the PEO subchain and $M_n = 7600$ for the PS subchain, respectively.

Binary Blends of Epoxy and PEO (and/or PS). It is necessary to know the miscibility and phase behavior of binary blends of epoxy with PEO (and/or PS) (viz., the subchains of the diblock copolymer) after and before curing to judge the mechanism of formation of the morphological structures in the thermosetting blends of epoxy and PS-*b*-PEO diblock copolymer. Before curing, PEO is miscible with the precursors of epoxy resin (viz., DGEBA and the curing agent).[35−37] After curing at elevated temperature, the ternary mixtures composed of DGEBA, MOCA, and PEO were gradually converted into the binary thermosetting blends of epoxy thermoset with PEO. The thermosetting blends displayed single, composition-dependent glass transition temperatures (T_g) in the entire composition as revealed by means of differential scanning calorimetry (DSC),[35] indicating that the miscible semi-interpenetrating polymer networks (semi-IPN) were formed after curing.[35,37] The miscibility of the thermosetting blends was attributed to the formation of the intermolecular hydrogen-bonding interactions between the hydroxyl groups of amine-cured epoxy and ether oxygen atoms of PEO in the thermosetting blends.[36−39]

To investigate the miscibility and phase behavior of the binary blends of epoxy and PS, it is necessary to prepare the PS with the identical molecular weight with the PS block length of the diblock copolymer. In this work, the length of PS block was taken as the value of molecular weight measured by ^{1}H NMR spectrocopy ($M_n = 12\,600$) other than that of GPC ($M_n = 15\,600$) because the former could be much closer than the theoratical molecular weight value.[40,41] The miscibility and phase beahvior after and before curing were investigated by phase contrast microscopy (PCM) and scanning electron microscopy (SEM). Before curing, all the PS/DGEBA blends were cloudy at room temperature. However, the blends became transparent

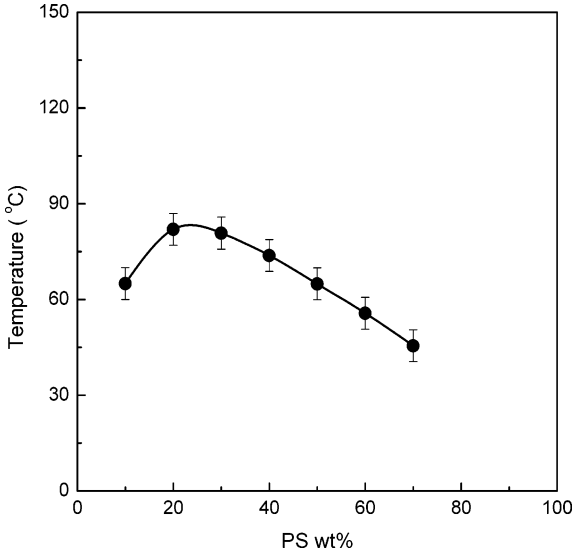

Figure 2. Cloud point curve of DGEBA/PS blends.

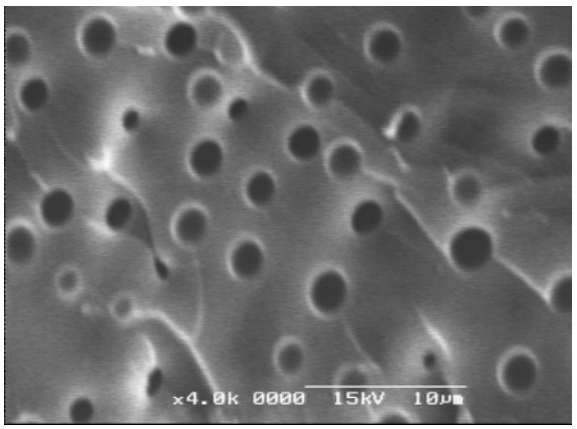

Figure 3. SEM micrograph of the epoxy thermosetting blend containing 10 wt % PS. The fracture end of the blend has been etched with tetrahydrofuran for 30 min.

when heated to elevated temperature (e.g., 90 °C), suggesting that the mixture possesses an upper critical solution temperature (UCST) behavior. By means of phase contrast microscopy, the cloud point curve of the blend system was determined as shown in Figure 2. It is seen that the blends displayed an asymmetric phase diagram, with the maximum critical solution temperature of ca. 82 °C for the mixture containing 20 wt % of PS. The cloud point curve is comparable to those reported in the literature.[42,43] The cloud point curve suggests that the thermosetting blends of epoxy with PS can be prepared from the initially homogeneous mixture while the curing temperature is above the UCST of the system. With addition of the curing agent (viz., MOCA) to the system, the blends were cured at 150 °C for 4 h to access a complete curing reaction. It was noted that, with the curing reaction proceeding, the initially transparent mixtures gradually became cloudy, indicating that the reaction-induced phase separation occurred in the binary thermosetting blends. The fractured ends of the cured blends were subjected to scanning electron microscopy (SEM) for morphological observation. The SEM micrograph of the blend containing 10 wt % of PS was representatively presented in Figure 3. To observe the morphology clearly, tetrahydrofuran (THF) was used as the solvent to rinse the PS phase, while the epoxy phase remained unaffected. It is seen that a heterogeneous morphology was obtained after the fractured end was etched. The spherical holes were ascribed to PS phase, and thus the

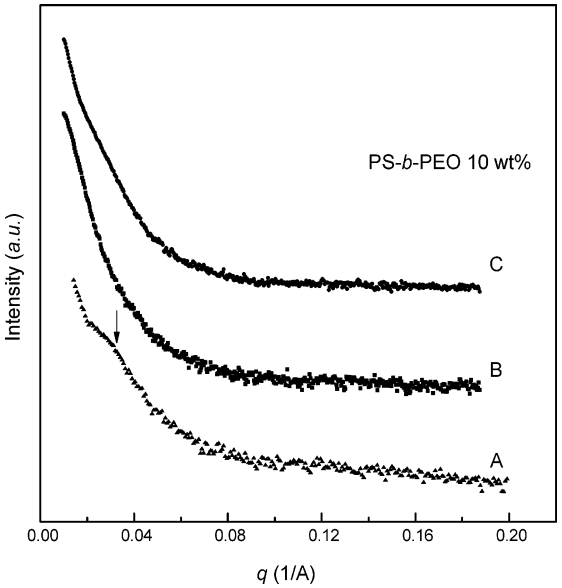

Figure 4. SAXS profiles of the blends of epoxy precursors with 10 wt % PS-*b*-PEO diblock copolymer: (A) DGEBA/PS-*b*-PEO blend at room temperature; (B) DGEBA + MOCA/PS-*b*-PEO at room temperature, (C) DGEBA + MOCA/PS-*b*-PEO at the beginning of curing reaction (viz., at 150 °C).

spherical PS particles (2−5 μm in diameter) were dispersed uniformly in the continuous epoxy matrix. The SEM result indicates that the reaction-induced phase separation occurred in the thermosetting blends of epoxy and PS.

Formation of Ordered Nanostructures in Epoxy Thermosets. In terms of the miscibility and phase behavior of the above binary thermosetting blends of epoxy resin with PEO (and/or PS), it is plausible to propose that the reaction-induced microphase separation would occur in the thermosetting blends of epoxy resin and PS-*b*-PEO diblock copolymer while the curing reaction is carried out at the temperature higher than the UCST of epoxy monomers and the PS blends, i.e., the PS subchains can be separated out with the curing reaction proceeding, whereas the PEO subchains remain miscible with the crosslinked epoxy matrix. Therefore, the nanostructured epoxy thermosets can be obtained.

Before curing, all the mixtures composed of DGEBA, MOCA, and PS-*b*-PEO were transparent, suggesting that the mixtures were homogeneous and no macroscopic phase separation occurred at the scale more than the wavelength of visible light. It should be pointed out that the homogeneity of the ternary mixtures does not necessarily preclude the presence of self-organized nanostructures at room temperature because it has been shown that the blends of DGEBA with PS displayed an upper critical solution temperature (UCST) behavior. To examine the possible presence of the self-organized nanostructures prior to curing, the phase behavior of the blends was examined by small-angle X-ray scattering (SAXS) at room temperature and at the beginning of the curing reaction. Figure 4 representatively presents the SAXS profiles of the mixtures containing 10 wt % of PS-*b*-PEO. At room temperature, the binary mixture of DGEBA and PS-*b*-PEO exhibited showed a peak at ca. $q = 0.03$ Å^{-1}, corresponding to a long period of 20.9 nm (see curve A), suggesting that the mixture is microphase-separated. It is believed that the micelle structure is formed in the mixture because DGEBA behaves as the selective solvent of the diblock copolymer. It is worth noticing that, upon adding equimolar MOCA (viz., the curing agent), the micelle structure disappeared, which was evidenced by the SAXS result of the ternary mixture of DGEBA, MOCA, and PS-*b*-PEO. It is observed that no scattering peak was displayed in the SAXS profile of the ternary mixture at room temperature (see curve B). This observation indicates that, at room temperature, the mixture composed of DGEBA, MOCA, and PS-*b*-PEO is homogeneous at the nanometer scale although the binary blends of DGEBA and PS-*b*-PEO are phase-separated. The behavior of miscibility could be attributed to the change in solubility parameter resulting from the inclusion of equimolar MOCA. This result is in a good agreement with the fact that the ternary blends composed of DGEBA, MOCA, and PS are homogeneous at room temperature. When the sample was heated to 150 °C (viz., the curing temperature), there was also no discernible scattering peak in the SAXS scattering profile of the blend (see curve C). This observation is important to indicate that no preformed nanostructures were formed at the beginning and that the samples were cured at the elevated temperature. Therefore, if there are any nanostructures that exist in the cured blends, they must be formed by a reaction-induced microphase separation process other than the self-assembly mechanism.[12,13]

All of the thermosetting blends of epoxy with PS-*b*-PEO were cured at 150 °C for 2 h plus 180 °C for 2 h to access complete curing reactions. In the present work, the contents of PS-*b*-PEO in thermosets were changed from 10 to 50 wt %, corresponding to the concentration of PS from 6 to 30 wt %, respectively, in the thermosets. All of the cured blends were transparent, indicating no macroscopic phase separation of epoxy and the block copolymer in the final cured states. The morphologies of the cured thermosets were investigated by atomic force microscopy (AFM). The AFM images of the thermosets containing 10, 20, 30, and 40 wt % of the PS-*b*-PEO are presented in Figure 5. Shown in the left-hand side of each micrograph are the topography images, and in the right are the phase images. The height images showed that the surfaces of the as-prepared specimens (ultrathin sections) are free of visible defects and quite smooth, and thus the effect of toughness resulting from the specimen preparation on morphology can be negligible. It is noted that all of the blends exhibited nanostructured morphologies. In terms of the volume fraction of PS and the difference in viscoelastic properties between epoxy and PS phases, the light continuous regions are ascribed to the crosslinked epoxy matrix, which could be interpenetrated by the PEO blocks of the copolymer, while the dark regions are attributed to PS domains. It is observed that, for the blend containing 10 wt % of PS-*b*-PEO, the nanosized PS spherical particles with the size of 10−20 nm were homogeneously dispersed into the continuous epoxy matrix. With increasing the content of PS-*b*-PEO, some interconnected PS microdomains began to appear (Figure 5C) and the quantity of the PS microdomains was increased, whereas the size of the spherical particle remains almost invariant (Figure 5A−C). It is interesting to note that the ordered nanostructure can be seen even with bare eyes when the concentration of diblock copolymer is 40 wt % (Figure 5D). The morphologies of the thermosetting blends were further investigated by small-angle X-ray scattering (SAXS).

Shown in Figure 6 are the SAXS profiles of the thermosets containing 10, 20, 30, and 40 wt % of PS-*b*-PEO diblock copolymer. The well-defined scattering peaks were observed in all the cases, indicating that the thermosets containing PS-*b*-PEO are microphase-separated. It is noted that all the SAXS profiles exhibited the multiple scattering maxima as denoted with the arrows in Figure 6, indicating that the thermosets could possess long-range ordered microstructures. From the relative positions of the scattering maxima, it is judged that the ordered

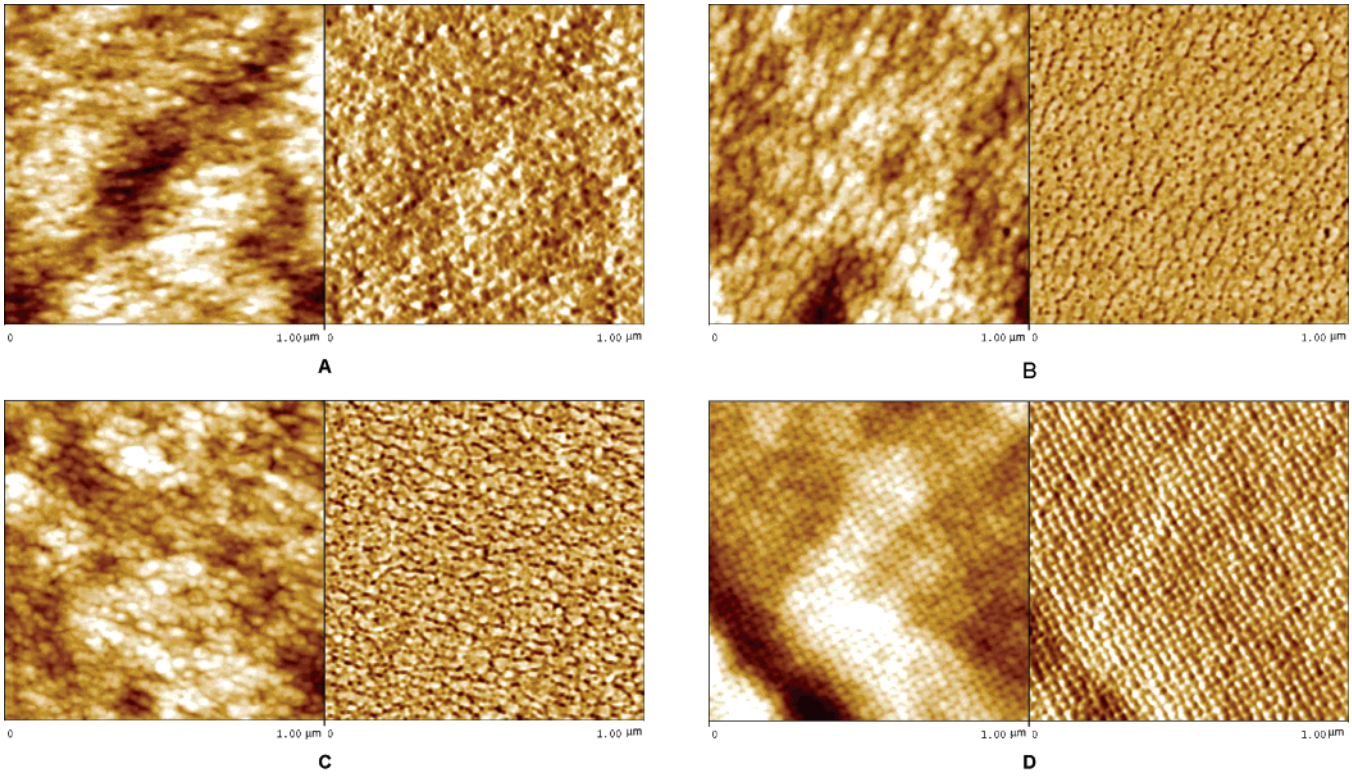

Figure 5. AFM images of the thermosets containing 10, 20, 30, and 40 wt % of PS-*b*-PEO diblock copolymer. Left: topography; right: phase contrast images.

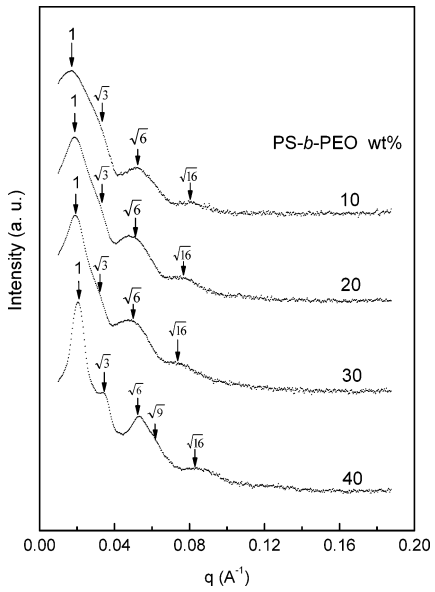

Figure 6. SAXS profiles of the epoxy thermosets containing PS-*b*-PEO diblock copolymer of: (A) 10, (B) 20, (C) 30, and 40 wt %.

nanophases were accessible to the epoxy thermosets containing PS-*b*-PEO diblock copolymer. The positions of the scattering maxima remain essentially constant, apart from slight shifts to the higher q values with increase in the content of PS-*b*-PEO. This observation could be associated with local rearrangement leading to an enhancement of the long-range order. The scattering peaks of the thermosets are situated at q values of 1, $3^{0.5}$, $6^{0.5}$ (or $7^{0.5}$), $9^{0.5}$,$12^{0.5}$, and $16^{0.5}$ relative to the first-order scattering peak positions (q_m). It is plausible to propose that these are the lattice scattering peaks of spherical (or cylindrical) nanophases arranged in cubic lattices such as body-centered cubic (bcc), face-centered cubic (fcc), or simple cubic symmetries. In addition, hexagonally packed cylinder morphology is also possible. It should be pointed out that it is not easy unambiguously to judge the types of packing lattices only in terms of SAXS profiles for the thermosetting blends containing 10, 20, and 30 wt % PS-*b*-PEO because the scattering peaks are quite broad, i.e., the ordering is apparently not good enough. Nonetheless, it is of interest to note that the packing lattice of the blend containing 40 wt % PS-*b*-PEO could be a simple cubic symmetry according to the AFM result (Figures 5D and 10) and the SAXS profile. The values of q_m give access to the Bragg spacing of the lattices according to the equation $L = 2\pi/q_m$, and the values of $d_m = 37.4$, 33.4, 32.5, and 31.2 nm were obtained for the thermosets containing the block copolymer of 10, 20, 30, and 40 wt %, respectively. The values of d_m correspond to the average distance between neighboring domains. It is noted that the average distance between neighboring domains decreased with increase of the content of the diblock copolymer. These results are in a good agreement with those obtained by means of AFM.

Formation Mechanism of Ordered Nanostructures. The nanostructures in the thermosets were formed via selective microphase separation of PS subchains induced by polymerization other than by fixing preformed self-assembly nanophases in the mixtures of the diblock copolymer and the epoxy precursors. The driving force for the reaction-induced microphase separation of PS blocks is the decrease in entropic contribution to free energy of mixing with the occurrence of cross-linking reactions. However, the PEO blocks are miscible with the cross-linked epoxy networks, i.e., the subchains of PEO could be interpenetrated into the cross-linked epoxy network at the segmental level. The interpenetration of PEO subchains into the epoxy networks can be further demonstrated by the depression in glass transition temperatures (T_g's) for the epoxy matrixes.

The DSC thermographs of the nanostructured epoxy thermosets are shown in Figure 7. The glass transition temperature

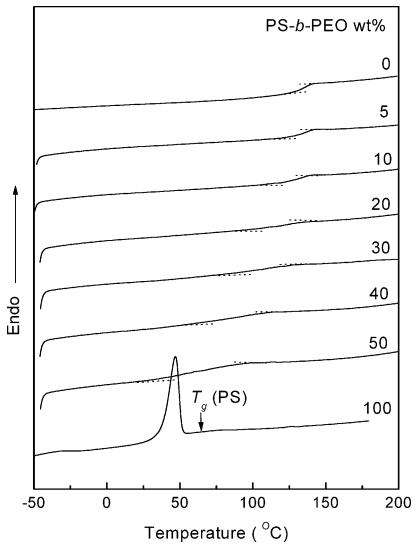

Figure 7. DSC curves of the nanostructured epoxy thermosets.

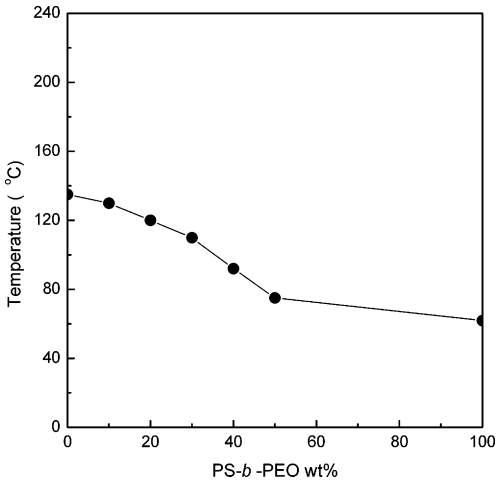

Figure 8. Plot of glass transition temperatures (T_g's) as a function of PS-*b*-PEO content.

(T_g) of the control epoxy is about 135 °C. The curve of PS-*b*-PEO diblock copolymer displays a sharp melting transition at ca. 55 °C and a glass transition at ca. 67 °C. The melting transition is ascribed to the crystalline PEO subchain, whereas the glass transition is responsible for the PS subchains. The fact that the melting transition of PEO subchains appears prior to the glass transition of PS subchains indicates that the diblock copolymer is microphase separated. It is noted that all the thermosets investigated did not exhibit the melting transition of PEO subchains, suggesting that the PEO subchains are not crystalline in the nanostructured thermosets. It is plausible to propose that the PEO subchains were interpenetrated in the cross-linked epoxy networks, i.e., the PEO subchains are miscible with the epoxy networks. The behavior of miscibility was further confirmed by the depression in glass transition temperatures (T_g's) for the epoxy-rich phases, as shown in Figure 8. This result is in good agreement with the miscible binary thermosetting blend of MOCA-cured epoxy with PEO.[35] In addition, it is worth noticing that the width of the glass transition region for the nanostructured thermosets is significantly higher than that of control epoxy. The broadening of the glass transition range could be attributed to the enrichment of soft PEO chains around the PS microdomains, i.e., only the cross-linked epoxy matrixes near the front of PS domains were efficiently plasticized by PEO chains and exhibited lower glass transition

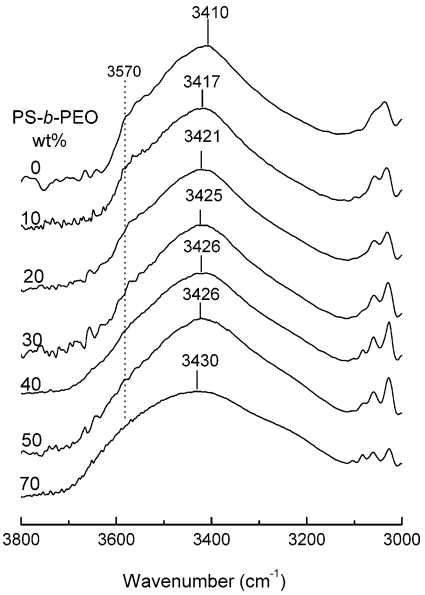

Figure 9. FTIR spectra of the nanostructured thermosets in the range of 4000−3000 cm^{-1}.

temperatures (T_g's) than the epoxy matrixes that were not interpenetrated by PEO blocks. The miscibility is ascribed to the formation of the intermolecular hydrogen-bonding interactions between aromatic amine cross-linked epoxy and PEO, which is readily evidenced by Fourier transform infrared spectroscopy (FTIR). Shown in Figure 9 are the FTIR spectra of the epoxy thermosets containing PS-*b*-PEO in the range of 4000−3000 cm^{-1}. The broad bands were attributed to the stretching vibration of the self-associated hydroxyls, the width of which reflects the wide distribution of hydrogen-bonded hydroxyl stretching frequencies. For the control epoxy, the stretching vibration of the self-associated hydroxyl groups (viz., −OH···−OH) occurred at 3410 cm^{-1} and that of free hydroxyl groups occurs at 3570 cm^{-1}.[44,45] Upon adding PEO to the system, it was noted that a part of hydroxyl stretching vibration shifted to the higher frequencies (e.g., 3426 cm^{-1} for the blend containing 40 wt % PS-*b*-PEO), i.e., the hydroxyl bands were increasingly broadened due to the presence of the components at the higher frequencies. The shifts of hydroxyl stretching vibration bands to the higher frequencies are an indicative of the formation of the intermolecular hydrogen-bonding interactions between epoxy networks and PEO subchains, which are stronger than the self-association of hydroxyl groups with the cross-linked epoxy networks.[46−50]

In view of the difference in miscibility and phase behavior in the blends of the subchains (i.e., PS and PEO) of the diblock copolymer with the cured epoxy after and before curing, the formation mechanism of the nanostructures in the thermosets was proposed as illustrated in Scheme 2. At the beginning of the curing reaction, all the subchains (viz., PEO and PS) of the diblock copolymer are miscible with the precursors (viz., DGEBA and MOCA) of epoxy at 150 °C, i.e., no self-assembly structures were formed at the beginning of the curing reaction. With the curing reaction proceeding, the PS subchains were separated out at the nanoscale, whereas the PEO subchains remained in the cross-linked epoxy networks. The microphase separation of the PS block was driven by the increased molecular weight of the system due to polymerization.

The above mechanism could be used well to interpret the formation of the microstructures at the nanometer scale. Nonetheless, the question is still present why the long-range ordered structures can be accessed via the reaction-induced

Scheme 2. Formation of Nanostructures in Epoxy Thermosets Containing PS-*b*-PEO Diblock Copolymer

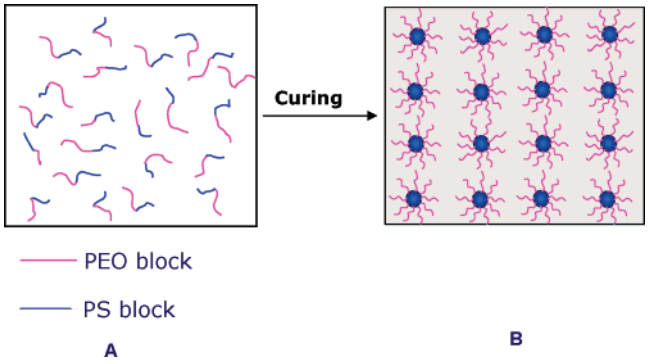

microphase separation mechanism. Obviously, the formation of the ordered nanostructures is quite different from that of equilibrium ordered (or disordered) self-assembly nanophases in the mixture with precursors of thermosets with amphiphilic block copolymers.[14−28] In the former case, the process of microphase separation induced by polymerization was carried out under the nonequilibrium condition. As the curing reaction proceeded, the blend system of in situ polymerization underwent a series of structural changes involving chain extension, branching, and cross-linking in succession; the system was gradually converted from the homogeneous solution into the three-dimensional networks due to the occurrence of gelation. It is proposed that, in the thermoset blends of epoxy with a homopolymer (or random copolymer), the formation of phase-separated morphology is governed by the competitive kinetics between polymerization and phase separation. The mechanism of spinodal decomposition (SD) (and/or nucleation and growth, NG) induced by polymerization results in the formation of very fine phase-separated structures at the micrometer scale.[1,2] While an amphiphilic diblock copolymer is used instead of the homopolymer (and/or random copolymer), phase separation would perform in a confined manner. In the present case, the PEO subchains of the diblock copolymer are miscible with the epoxy matrix, and thus the growth of PS domains will be confined to the nanometer scale. The macroscopic phase separation is thus suppressed by the presence of the PEO subchains, which depress the surface free energy of PS particles. It is worth noticing that the size distribution of the PS microdomains obtained is quite uniform. It is plausible to propose that the ordered nanostructures can be formed if the uniformly distributed PS microdomains were densely packed. In the present case, the PS microdomains were found to pack into a long-range ordered cubic lattice for the thermosetting blend containing 40 wt % of PS-*b*-PEO, as shown in Figure 10. The formation mechanism of the ordered nanostructure is in marked contrast to the mechanism of self-assembly of block copolymer in precursors of thermosets together with subsequent fixation of the self-organized structures.

Conclusions

The amphiphilic diblock copolymers, polystyrene-*b*-poly(ethylene oxide) (PS-*b*-PEO), were synthesized via the atom transfer radical polymerization (ATRP) of styrene with 2-bromoisobutyryl-terminated PEO monomethyl ether [PEO−OOCCBr$(CH_3)_2$] as the macroinitiator. The diblock copolymers were characterized by Fourier transform infrared spectroscopy (FTIR), nuclear magnetic resonance spectroscopy (NMR), and gel permeation chromatography (GPC). The PS-*b*-PEO diblock copolymers were used to incorporate into epoxy resin to afford

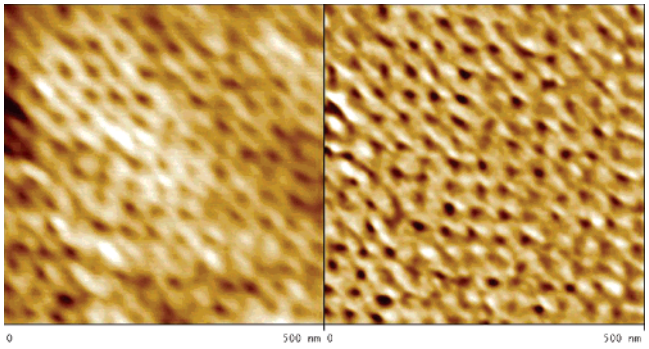

Figure 10. Enlarged AFM images of the thermoset containing 40 wt % of PS-*b*-PEO diblock copolymer image. Left: topography; right: phase contrast image.

the nanostructured epoxy thermosets. Both atomic force microscopy (AFM) and small-angle X-ray scattering (SAXS) show that the long-range ordered nanostructures were obtained based on the protocol of curing. It is found that the nanophases of PS were found to arrange into simple cubic symmetry lattices while the content of diblock copolymer was 40 wt %. In view of the difference in miscibility and phase behavior for the blends of the subchains (i.e., PS and PEO) of the diblock copolymer with the cured epoxy after and before curing, the formation mechanism of the ordered nanostructures in the thermosets was proposed to be via the reaction-induced microphase separation, which is in marked contrast to the mechanism of self-assembly of block copolymers thermosets together with the subsequent fixation of the self-organized structures.

Acknowledgment. The financial support from the Natural Science Foundation of China (project nos. 20474038 and 50390090) are acknowledged. S.Z. thanks the Shanghai Educational Development Foundation, China, under an award (2004-SG-18) to the "Shuguang Scholar".

References and Notes

(1) Pascault, J. P.; Williams R. J. J. In *Polymer Blends*; Paul, D. R., Bucknall, C. B., Eds.; Wiley: New York, 2000; Vol. 1, pp 379.
(2) Guo, Q. In *Polymer Blends and Alloys*; Shonaik, G. O., Simon, G., Eds.; Marcel Dekker: New York, 1999; Chapter 6, pp 155.
(3) de Gennes, P.-G. *Scale Concepts in Polymer Physics*; Cornell University Press: Ithaca, NY, 1979.
(4) de Gennes, P.-G. *Phys. Lett. A* **1969**, *28*, 725.
(5) Barclay, G. G.; Ober, C. K.; Papathomas, K. I.; Wang, D. W. *Macromolecules* **1992**, *25*, 2947.
(6) Boer, D. J.; Lun, J.; Mol, G. N. *Macromolecules* **1993**, *26*, 1244.
(7) Litt, M. H.; Whang, W.-T.; Yen, K.-T.; Qian, X.-J. *J. Polym. Sci., Part A: Polym. Chem.* **1993**, *31*, 183.
(8) Hikmet, R. A. M. *Macromolecules* **1992**, *25*, 5759.
(9) Hikmet, R. A. M.; Lub, J.; Higgins, J. A. *Polymer* **1993**, *34*, 1736.
(10) Kishore, G. K. *Macromolecules* **1993**, *26*, 2995.
(11) Lin, Q.; Yee, A. F.; Earls, J. D.; Hefner, R. E.; Sue, H.-J. *Polymer* **1994**, *35*, 2679.
(12) Hillmyer, M. A.; Lipic, P. M.; Hajduk, D. A.; Almdal, K.; Bates, F. S. *J. Am. Chem. Soc.* **1997**, *119*, 2749.
(13) Lipic, P. M.; Bates, F. S.; Hillmyer, M. A. *J. Am. Chem. Soc.* **1998**, *120*, 8963.
(14) Mijovic, J.; Shen, M.; Sy, J. W.; Mondragon, I. *Macromolecules* **2000**, *33*, 5235.
(15) Guo, Q.; Thomann, R.; Gronski, W. *Macromolecules* **2002**, *35*, 3133.
(16) Guo, Q.; Thomann, R.; Gronski, W. *Macromolecules* **2003**, *36*, 3635.
(17) Ritzenthaler, S.; Court, F.; Girard-Reydet, E.; Leibler, L.; Pascault, J. P. *Macromolecules* **2002**, *35*, 6245.
(18) Ritzenthaler, S.; Court, F.; Girard-Reydet, E.; Leibler, L.; Pascault, J. P. *Macromolecules* **2003**, *36*, 118.
(19) Kosonen, H.; Ruokolainen, J.; Nyholm, P.; Ikkala, O. *Macromolecules* **2001**, *34*, 3046.
(20) Kosonen, H.; Ruokolainen, J.; Nyholm, P.; Ikkala, O. *Polymer* **2001**, *42*, 9481.

(21) Kosonen, H.; Ruokolainen, J.; Torkkeli, M.; Serimaa, R.; Nyholm, P.; Ikkala, O. *Macromol. Chem. Phys.* **2002**, *203*, 388.
(22) Grubbs, R B.; Dean, J. M.; Broz, M. E.; Bates, F. S. *Macromolecules* **2000**, *33*, 9522.
(23) Rebizant, V.; Abetz, V.; Tournihac, T.; Court, F.; Leibler, L. *Macromolecules* **2003**, *36*, 9889.
(24) Dean, J. M.; Verghese, N. E.; Pham, H. Q.; Bates, F. S. *Macromolecules* **2003**, *36*, 9267.
(25) Rebizant, V.; Venet, A. S.; Tournillhac, F.; Girard-Reydet, E.; Navarro, C.; Pascault, J. P.; Leibler, L. *Macromolecules* **2004**, *37*, 8017.
(26) Dean, J. M.; Grubbs, R. B.; Saad, W.; Cook, R. F.; Bates, F. S. *J. Polym. Sci., Part B: Polym. Phys.* **2003**, *41*, 2444.
(27) Wu, J.; Thio, Y. S.; Bates, F. S. *J. Polym. Sci., Part B: Polym. Phys.* **2005**, *43*, 1950.
(28) Guo, Q.; Dean, J. M.; Grubbs, R. B.; Bates, F. S. *J. Polym. Sci., Part B: Polym. Phys.* **2003**, *41*, 1994.
(29) Flory, P. J. *Principles of Polymer Chemistry*; Cornell University Press: Ithaca, NY, 1953.
(30) Meng, F.; Zheng, S.; Zhang, W.; Li, H.; Liang, Q. *Macromolecules* **2006**, *39*, 711.
(31) Wang, J.-S.; Matyjaszewski, K. *J. Am. Chem. Soc.* **1995**, *117*, 5614.
(32) Le, T. P.; Moad, G.; Rizzardo, E.; Thang, S. H. PCT Int. Appl. WO 98/01478, 1998.
(33) Jnkova, K.; Chen, X.; Kops, J.; Batsberg, W. *Macromolecules* **1998**, *31*, 538.
(34) Tanaka, H.; Nishi, T. *Phys. Rev. A* **1989**, *39*, 783.
(35) Yin, M.; Zheng, S. *Macromol. Chem. Phys.* **2005**, *206*, 929.
(36) Luo. X.; Zheng, S.; Zhang, N.; Ma, D. *Polymer* **1994**, *35*, 2619.
(37) Zheng, S.; Zhang, N.; Luo, X.; Ma, D. *Polymer* **1995**, *36*, 3609.
(38) Horng, T. J.; Woo, E. M. *Polymer* **1998**, *39*, 4115.
(39) Guo, Q.; Harrats, C.; Groeninckx, G.; Koch, M. H. J. *Polymer* **2001**, *42*, 4127.
(40) Cai, Y.; Armes, S. P. *Macromolecules* **2005**, *38*, 271.
(41) Zhang, H.; Sun, X.; Wang, X.; Zhou, Q.-F. *Macromol. Rapid Commun.* **2005**, *26*, 407.
(42) Hoppe, C. E.; Galante, M. J.; Oyanguren, P. A.; Willams, R. J. J.; Girard-Reydet, E.; Pascault, J. T. *Polym. Eng. Sci.* **2002**, *42*, 2361.
(43) Zucchi, I. A.; Galante, M. J.; Borrajo, J.; Williams, R. J. J. *Macromol. Chem. Phys.* **2004**, *205*, 676.
(44) Coleman, M. M.; Painter, P. C. *Prog. Polym. Sci.* **1995**, *20*, 1.
(45) Coleman, M. M.; Graf, J. F.; Painter, P. C. *Specific Interactions and the Miscibility of Polymer Blends*; Technomic Publishing: Lancaster, PA, 1991.
(46) Hu, Y.; Motze, H. R.; Etxeberria, A. M.; Fernandez-Berridi, H. J.; Iruin, J. J.; Painter, P. C.; Coleman, M. M. *Macromol. Chem. Phys.* **2000**, *201*, 705.
(47) Coleman, M. M.; Moskala, E. J. *Polymer* **1983**, *24*, 251.
(48) Zheng, S.; Zheng, H.; Guo, Q. *J. Polym. Sci., Part B: Polym. Phys.* **2003**, *41*, 1085.
(49) Zheng, S.; Guo, Q.; Chan, C.-M. *J. Polym. Sci., Part B: Polym. Phys.* **2003**, *41*, 1099.
(50) Ni, Y.; Zheng, S. *Polymer* **2005**, *46*, 5828.

MA060004+